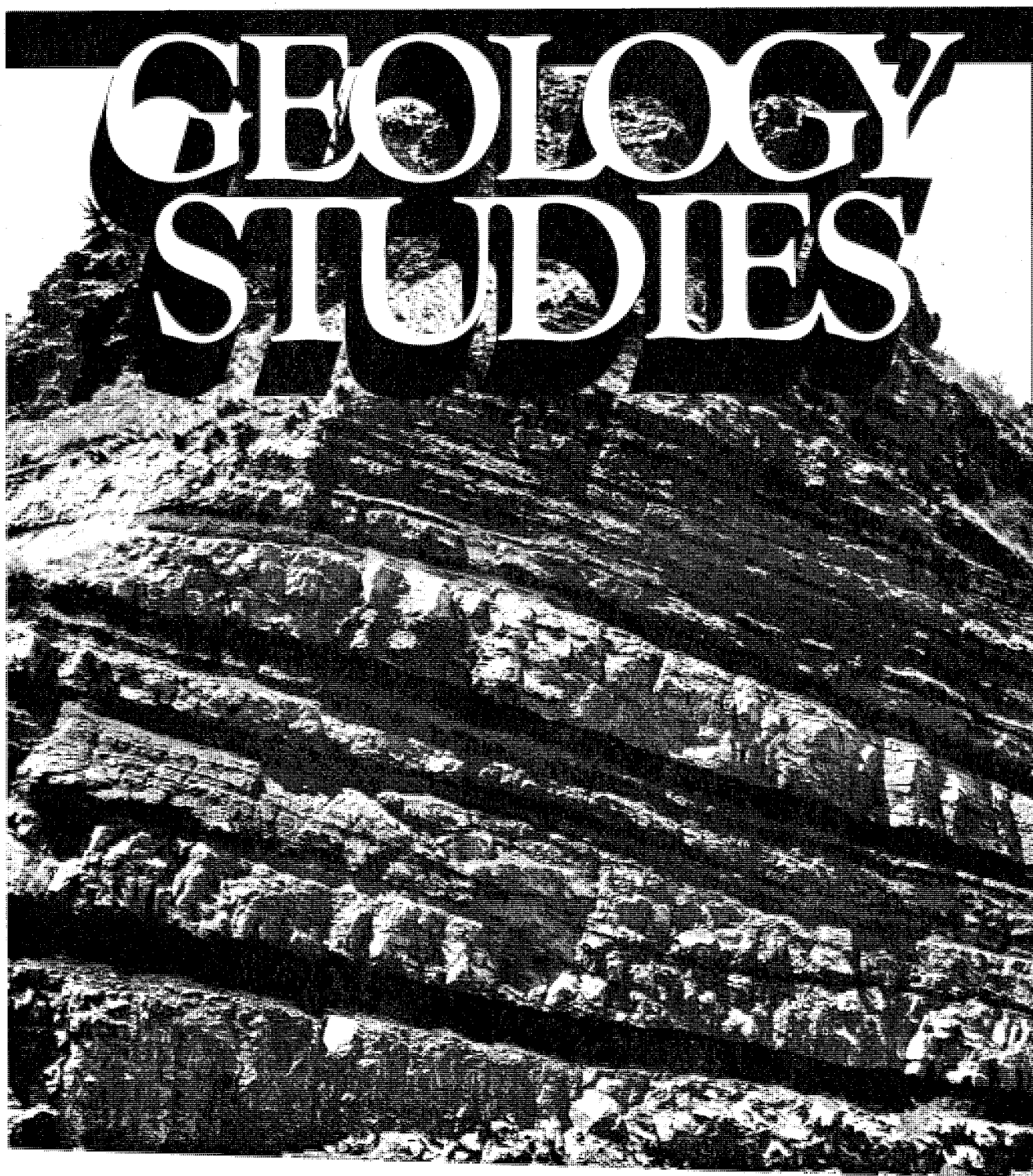


BRIGHAM YOUNG UNIVERSITY

GEOLOGY STUDIES



VOLUME 26, PART 2

JULY 1979

Brigham Young University Geology Studies

Volume 26, Part 2

CONTENTS

A New Large Theropod Dinosaur from the Upper Jurassic of Colorado.....	Peter M. Galton and James A. Jensen
Preliminary Zonations of Lower Ordovician of Western Utah by Various Taxa.....	Lehi F. Hintze
Environmental Significance of Pterosaur Tracks in the Navajo Sandstone (Jurassic), Grand County, Utah.....	William Lee Stokes and James H. Madsen, Jr.
Stratigraphy and Archaeocyathans of Lower Cambrian Strata of Old Douglas Mountain, Stevens County, Washington.....	George L. Hampton III
Thermoluminescence Dating of Quaternary Basalts: Continental Basalts from the Eastern Margin of the Basin and Range Province, Utah and Northern Arizona.....	Richard D. Holmes
Upper Devonian and Lower Mississippian Strata on the Flanks of the Western Uintas.....	W. Carl Spreng
Sedimentary Environment of the Cretaceous Ferron Sandstone near Caineville, Utah.....	Jack Uresk
Carbonate Mud Mounds from the Lower Ordovician Wah Wah Limestone of the Ibex Area, Western Millard County, Western Utah.....	Danny J. Wyatt

Publications and Maps of the Geology Department



Cover: Cretaceous coals near Castle Gate, Utah.

A publication of the
Department of Geology
Brigham Young University
Provo, Utah 84602

Editors

W. Kenneth Hamblin
Cynthia M. Gardner

Brigham Young University Geology Studies is published by the department. *Geology Studies* consists of graduate-student and staff research in the department and occasional papers from other contributors. *Studies for Students* supplements the regular issues and is intended as a series of short papers of general interest which may serve as guides to the geology of Utah for beginning students and laymen.

ISSN 0068-1016

Distributed July 1979

7-79 525 38477

CONTENTS

A NEW LARGE THEROPOD DINOSAUR FROM THE UPPER JURASSIC OF COLORADO	1	Abstract	21
Abstract	1	Introduction	21
Introduction	1	Navajo Sandstone	21
Acknowledgments	1	Geologic setting of the Sand Flats locality	21
Systematic section	1	Postulated sequence of events	23
Description and comparisons	4	Modern analogy	23
Humerus, radius, ulna	4	Petrology	24
Manus	4	Discussion and conclusions	25
Pelvic girdle	6	Acknowledgments	26
Discussion	8	References cited	26
References cited	11	Figures	
Figures		1. Discovery site of pterosaur tracks	21
1. Humerus, radius, and ulna	2	2. Near view of remnant on ridge above discovery site	22
2. Articulated forelimb and pelvic girdle	3	3. One of two track-marked slabs in place of discovery	22
3. Forelimbs of saurischian dinosaurs	5	4. Photomicrograph: Hematite-cemented sandstone	23
4. Manus	6	5. Photomicrograph: Track-bearing sandstone	24
5. Prosauropod manus-digit I	7	6. Near view of track-marked surface	25
6. Ilium and pubis	8,9		
7. Articulated pelvic girdle	10	STRATIGRAPHY AND ARCHAEOCYATHANS OF LOWER CAMBRIAN STRATA OF OLD DOUGLAS MOUNTAIN, STEVENS COUNTY, WASHINGTON	27
8. Pelvic girdles of saurischian dinosaurs	11	Introduction	27
Tables		Location	27
1. Measurements of figured forelimb bones	4	Previous work	27
2. Ratios for forelimb bones of carnosaurian theropods	4	Methods	28
		Stratigraphy	28
PRELIMINARY ZONATIONS OF LOWER ORDOVICIAN OF WESTERN UTAH BY VARIOUS TAXA	13	Gypsy Quartzite	29
Abstract	13	Maitlen Formation	29
Introduction	13	Structure	32
Trilobite zones	13	Paleontology of carbonate units	33
Conodont zones	14	Systematic paleontology	33
Graptolite zones	15	Introductory remarks	33
Cephalopod zones	15	Classification	34
Other fossil groups	16	Systematics	34
Summary	17	Conclusions	38
Annotated reference list	18	Acknowledgments	38
Figures		References cited	39
1. Geologic map of Utah	13	Figures	
2. Trilobite zones in western Utah	14	1. Index map	27
3. Ranges of conodonts form-species	14	2. View of Douglas Lake	28
4. Preliminary conodont zones/geologic formations	14	3. Geologic map	30
5. Graptolite zones/trilobite zones	15	4. Correlation chart	31
6. Ranges of brachiopod species	15	5. Stratigraphic column of study area	32
7. Brachiopod zones/trilobite zones	15	6. Fossil detritus lens	33
8. Inarticulate brachiopod occurrences	16	7. Drag folds	34
9. Cephalopod occurrences	16	Plates	
10. Gastropod occurrences	16	1. Trilobites, sponges, echinoderm plates, bryozoan(?), archaeocyathans.	41
11. Sponge occurrences	16	2. Archaeocyathan fauna	43
12. Ostracod occurrences	17	3. Archaeocyathan fauna	45
13. Echinoderm occurrences	17	4. Archaeocyathan fauna	47
14. Occurrences of bryozoa, pelecypods, and corals	17	5. Archaeocyathan fauna	49
ENVIRONMENTAL SIGNIFICANCE OF PTEROSAUR TRACKS IN THE NAVAJO SANDSTONE (JURASSIC), GRAND COUNTY, UTAH	21	THERMOLUMINESCENCE DATING OF QUATERNARY BASALTS: CONTINENTAL BASALTS FROM THE EASTERN MARGIN OF THE BASIN	

AND RANGE PROVINCE, UTAH AND NORTH-ERN ARIZONA

Abstract	51
Introduction	51
TL samples: Collection and preparation	51
Radioelement determination and dose rate calculations ...	52
Radioelement determinations	53
Dose rate calculations	54
TL measurements	55
Specific TL calculations and TL age dating	56
Petrochemical variations	56
Specific TL ratio calculations	58
Discussion of the TL results	60
Summary and conclusions	61
Acknowledgments	62
Appendix	62
References cited	64

Figures

1. Index map, western United States	52
2. Feldspar compositions: Ternary diagrams	52
3. Typical glow curves	56
4. Alkalies vs. silica variation diagram	58
5. Alumina vs. silica variation diagram	58
6. AFM variation diagram	58
7. Type I TL calibration	59
8. Type II TL calibration	59
9. Similar slopes of TL calibrations	61
10. Hypothetical development and saturation of TL ..	61

Tables

1. Microprobe analysis of feldspars	53
2. Interlaboratory comparison of U and Th determi- nations: Standard samples	53
3. Interlaboratory comparison of U and Th determi- nations: Basaltic samples	54
4. U, Th, and K ₂ O determinations	54
5. Dose rate calculations	55
6. TL measurements	57
7. Specific TL ratio calculations	60

UPPER DEVONIAN AND LOWER MISSISSIPPIAN STRATA ON THE FLANKS OF THE WESTERN UINTA MOUNTAINS, UTAH

Abstract	67
Introduction	67
Acknowledgments	67
Stratigraphy	67
General lithologic sequences	67
Nomenclature	68
Unconformities	70
Dolomitization	70
Rhythmic sedimentation	71
Method of investigation	73
Beaver Creek	73
South Fork	74
Smith and Morehouse Canyon	74
Gardner Fork	74
Duchesne River	74
Depositional history	75
Biostratigraphy	75
Summary	78
Addendum	78
References cited	78

Figures

1. Index map	67
2. Stratigraphic sections: Beaver Creek and South Fork	68
3. Composite stratigraphic section: Smith and Morehouse Canyon	69
4. Stratigraphic sections: Gardner Fork and Du- chesne River	70
5. Lithologic correlation diagram	71
6. Unconformable contact	72
7. Unconformable contact	72
8. Photomicrograph: Dolomitic pelsparite	73
9. Photomicrograph: Dolomicrite	73
10. Photomicrograph: Dolomicrite with stylolites	74
11. Map: Possible extensions of uppermost Devon- ian deposition	76
12. Ranges of selected megafauna	77

SEDIMENTARY ENVIRONMENT OF THE CRE-TACEOUS FERRON SANDSTONE NEAR CAIN-VILLE, UTAH

Abstract	81
Introduction	81
Location	81
Previous work	81
Methods	82
Acknowledgments	82
Geologic setting	82
Lithologies	83
Sandstone	83
Siltstone	86
Mudstone	86
Coal and carbonaceous shale	86
Other rock types	87
Fossils	87
Depositional significance of lithologies	87
Sandstone	87
Siltstone	88
Gray and green mudstone	88
Purple shale	88
Coal and carbonaceous shale	89
Ironstone	90
Economic possibilities	92
Coal	92
Uranium	93
Oil and gas	93
Titanium	93
Jet	93
Gravel	93
Depositional history	93
Observations	99
Coal quality and thickness	99
Conclusion	99
Appendix 1	99
Appendix 2	100
References cited	100

Figures

1. Index map	81
2. Measured section location map	83
3. Fence diagram	84
4. Geologic map	85
5. Normal fault related to subsidence	86
6. <i>Paraphyllanthoxylon</i> -like log in upper coal seam ...	87
7. Paleogeologic map of large sandstone	88

8. Sulfur concentration map	90	Fossil fragments	105
9. Flattened log	91	Pellets	105
10. Flattened log lacking woodlike structure	91	Intraclasts	105
11. Ironstone concretion with wood core	91	Spar filling	105
12. Ironstone concretion	91	Trace occurrences	105
13. In situ stump	92	Paleontology	105
14. Sandstone-ironstone transition	92	Particle size analysis	106
15. Abandoned channel-fill sequence	94	Interpretation	107
16. Lower coal isopach	94	Surrounding beds	107
17. Paleogeologic map of large channel above lower coal	95	Underlying beds	107
18. Paleogeologic map of channel-fill and splay above lower coal	95	Lateral beds	107
19. "Stray" coal isopach	95	Overlying beds	107
20. Middle coal isopach	95	Discussion	109
21. Small channel-fill sandstone	96	Depositional model and modern analog	109
22. Local structural feature east of measured section 40	96	Conclusions	111
23. Ironstone over sandstone north of measured section 12	96	Summary	113
24. Paleogeologic map of interval between middle coal and purple marker unit	97	Acknowledgments	113
25. Paleogeologic map of purple marker unit horizon	97	References cited	113
26. Paleogeologic map of small channels above purple marker horizon	97	Figures	
27. Paleogeologic map of later sequence of channels above purple horizon	98	1. Index map of study area	101
28. Paleogeologic map of upper coal isopach	98	2. Overall view of study area and lens horizon	102
29. Paleogeologic map of interval between upper coal and Blue Gate Shale	99	3. Drillings of lens interiors	102
		4. Lens 14 and measured sections	103
		5. Close view of lens 14	103
		6. Photomicrograph: spar-filled burrows and fossil debris	104
		7. Photomicrograph: Trilobites and brachiopods	104
		8. Photomicrograph: Mudstone, lens 14, 114-cm level	104
		9. Photomicrograph: Wackestone, lens 14, 127-cm level	104
		10. Photomicrograph: Mudstone showing burrow mottling	105
		11. Photomicrograph: Mottled mudstone, lens 14, 50-cm level	105
		12. Photomicrograph: Wackestone-packstone from exterior of lens 14	105
		13. Photomicrograph: Sponge fragment	105
		14. Textural classification of constituent elements, lens interiors	106
		15. Exterior, lens 17	107
		16. Map of study area lenses	108
		17. Composition of carbonate lenses	108
		18. Measured sections, lens-bearing horizon of study area	110
		19. Histograms: Percent of skeletal grains by 1-mm size intervals	112
		20. Photomicrograph: Mudstone, unit 3, section 14C	113
		21. Photomicrograph: Wackestone of unit 3, section 14C	113
CARBONATE MUD MOUNDS FROM THE LOWER ORDOVICIAN WAH WAH LIMESTONE OF THE IBEX AREA, WESTERN MILLARD COUNTY, WESTERN UTAH			
Abstract	101		
Introduction	101		
Location	101		
Geologic setting	101		
Methods	102		
Terminology	103		
Previous work	103		
Lithology	103		
Lens interior	103		
Description	103		
Composition of lenses	104		
Burrows	104		
Burrowed matrix	104		
Unburrowed matrix	105		

Thermoluminescence Dating of Quaternary Basalts: Continental Basalts from the Eastern Margin of the Basin and Range Province, Utah and Northern Arizona*

RICHARD D. HOLMES

Australia National University, P.O. Box 4, Canberra ACT2600, Australia

ABSTRACT.—The thermoluminescence (TL) technique was applied to the age dating of Quaternary continental basalts (< 0.5 m.y. old) from the western United States. A calibration curve relating TL to age was constructed, using 17 samples dated by the K-Ar or ^{14}C methods. TL measurements were made on plagioclase separates from the basaltic samples. Electron microprobe analysis showed that the plagioclase separates ranged in composition from oligoclase to bytownite ($\text{An}_{30}\text{--An}_{77}$); variations in plagioclase composition had no significant effect on the TL response. Because potassium present in these plagioclase feldspars makes a larger contribution to their annual radiation dose rate than does potassium incorporated into other mineral phases of the basalt, a "composite" dose rate was calculated to correct for variations in the K_2O content of the plagioclases.

Variations in basalt type and chemistry were shown to have a significant effect on the TL response of the samples studied. Therefore, it was necessary to divide the samples into three petrochemical types: olivine tholeiite basalts, alkalic basalts, and basaltic andesites. On a log-log plot of the specific TL ratio, R , vs. age, the three types showed similar slopes but had different intercepts. Ten basalts of unknown age from Utah and northern Arizona were dated by the TL method.

INTRODUCTION

Recent studies of the tectonic development of the Basin and Range Province have utilized measured offsets on radiometrically dated lava flows to estimate rates of fault displacement and of regional uplift (McKee and McKee 1972, Luchitta 1972, Best and Hamblin 1979). The abundant late Cenozoic lava flows of basaltic composition which occur along the margins of the Basin and Range Province provide numerous opportunities for such studies. However, the analytical uncertainties and imprecisions of conventional K-Ar dating prevent the accurate dating of basaltic rocks younger than about 0.3 m.y. Along the eastern margin of the Basin and Range there are a significant number of Quaternary basalts which are younger than this 0.3 m.y. lower limit. Therefore, the thermoluminescence (TL) method was investigated as a technique for the age dating of these very young basalts. This paper describes the thermoluminescence techniques used in this study. The geologic discussion of these results can be found elsewhere (Holmes and others 1978).

The general theory of TL dating and the detailed history of its archaeological and geological applications have been reviewed elsewhere and will not be discussed here. (See Cairns 1976; Aitken 1968, 1974; May 1975, 1977; Dalrymple and Doell 1970; and McDougall 1968.)

Thermoluminescence dating has been used in archaeology for the last 10–15 years as an important supplement to radiocarbon dating for the dating of pottery materials less than about 20,000 years old. May (1975, 1977; see also Berry 1973) showed that it was possible to date Hawaiian alkalic basalts by measuring the thermoluminescence observed in plagioclase separated from these rocks. His TL techniques yielded ages that were generally within $\pm 10\%$ of the K-Ar or ^{14}C dates for samples from 4,000 to 200,000 years old.

The present study represents an extension of the techniques developed by May in an attempt to develop a TL dating scheme for young basalts of continental origin. Seventeen samples of known age were used to construct calibration curves of TL vs. age in order to develop a "relative" dating technique (May 1977, 1975; Berry 1973; Aitken 1974, p. 95). Relative dating schemes, in order to establish the relationship of TL intensity to age, rely upon comparison to samples of known age which have been dated by the K-Ar or ^{14}C methods. In contrast, TL methods designed to give "absolute" ages require no such calibration samples and assume that the TL signal accumulated linearly and that there has been no TL leakage (Cairns 1976; Aitken 1968, 1974). Such absolute methods are unsuited to the dating of geological materials which are generally very much older than the archaeological samples for which these "absolute" techniques were developed (see, however, Hwang 1971; Hwang and Goksu 1971).

TL SAMPLES: COLLECTION AND PREPARATION

The 36 samples used in this study were collected in the summer and fall of 1976. Seventeen were of known age and were collected to serve as reference standards. Detailed description of each sample and literature references for those previously dated may be obtained from the author. An index map is shown in figure 1. An expanded index map of the Long Valley area can be found in Bailey and others (1976).

The 12 samples of known age which were taken from the Long Valley Caldera, California, and from Idaho were collected on the basis of the published and unpublished descriptions of their locations (see appendix). Because detailed field notes on the locations of the Long Valley samples were not available to us, it was deemed advisable to test the authenticity of the samples collected there by comparing their published K_2O contents and petrographic descriptions (Bailey and others 1976) with those obtained during this study. Two samples (R-LNG73G021 and R-LNG73G025) were rejected on these criteria, and indications were that the resampling of these flows was not accurate. Several other samples differed in reported K_2O content by as much as 0.10 wt.% and were statistically *not* equivalent when compared by Student's t -Test. However, it was judged that these variations could be due to systematic inter-laboratory variations in the potassium determinations or to intraflow lateral variations in K_2O content.

Each sample was crushed in a hardened steel jaw-crusher and separated into two size fractions, +25 mesh and -25 mesh. The +25 mesh portion provided samples for gamma-ray spectrometry (~ 400 g.) and for bulk rock analysis (appendix). The -25 mesh portion was the source for the plagioclase separated used in the TL measurements. The 325 to 400 mesh size frac-

*A thesis presented to the Department of Geology, Brigham Young University, in partial fulfillment of the requirements for the degree Master of Science, March 1978. Thesis committee chairman: Myron G. Best.

tion of the -25 mesh portion was separated by sieving through nylon and brass screens, and the plagioclase in this size fraction was separated using a Frantz isodynamic magnetic separator. This size fraction (325-400 mesh) was chosen, as suggested by May (1975), since it approximates the size of plagioclase crystals in basaltic rocks, in order to facilitate the comparison of our results. Microscopic examination of the separates showed that most samples were 95 percent or more plagioclase; the most common impurities were volcanic glass, polymineralic fragments of the basaltic groundmass, calcite, and zeolites. Although care was taken to collect the freshest possible samples, some samples did contain minor amounts of secondary calcite

and/or zeolites; such samples were washed in dilute hydrochloric acid to remove the carbonate material.

Microprobe analysis was performed on grain mounts of each separate to determine its purity and compositional range. Standardization was made by comparison to natural feldspars and synthetic standards of known composition. Thirty-three of the samples were effectively pure plagioclase, ranging compositionally from oligoclase to bytownite. Figure 2 illustrates the compositional range of selected samples. Three samples contained significant quantities of minerals other than plagioclase. The most common impurity in these three samples is anorthoclase feldspar, which comprises up to 40% of the impure separates. These samples gave anomalous and erratic TL results which could not be correlated to the TL results of pure samples of similar age. Therefore, the following samples containing more than 5% anorthoclase were rejected as being unsatisfactory for TL dating: Zion-20, Flg-1, and Flg-2.

The four basaltic andesites from the Cove Fort field, Utah, contain minor amounts of xenocrystic quartz (Clark 1977), which comprise 5-15% of the separates taken from these samples. These samples gave significantly different TL results from the other basaltic samples and were grouped separately for the analysis of TL results and the calculation of TL ages.

Table 1 shows the average composition and compositional range of each plagioclase separate. Although there are some variations between the composition of the separates from the several geographic areas and from rocks of somewhat varying basaltic composition, variation in plagioclase composition, within the range of oligoclase to bytownite, does not seem to be an important parameter controlling the TL response of the samples. This conclusion supports earlier similar findings reported by May (1975, 1977) and by Garlick and others (1971, p. 2279). However, it was noted that variations in the K_2O content of the plagioclase (expressed as wt.% orthoclase in table 1) could significantly affect the effective radiation dose rate received by the plagioclase crystals (see below).

RADIOELEMENT DETERMINATIONS AND DOSE RATE CALCULATIONS

The accurate determination of the average annual radiation dose received by the plagioclase dosimeter crystals is of key importance to the construction of an accurate TL dating scheme. Dose rates are usually calculated from the chemically determined concentrations of the long-lived radionuclides (^{238}U ,

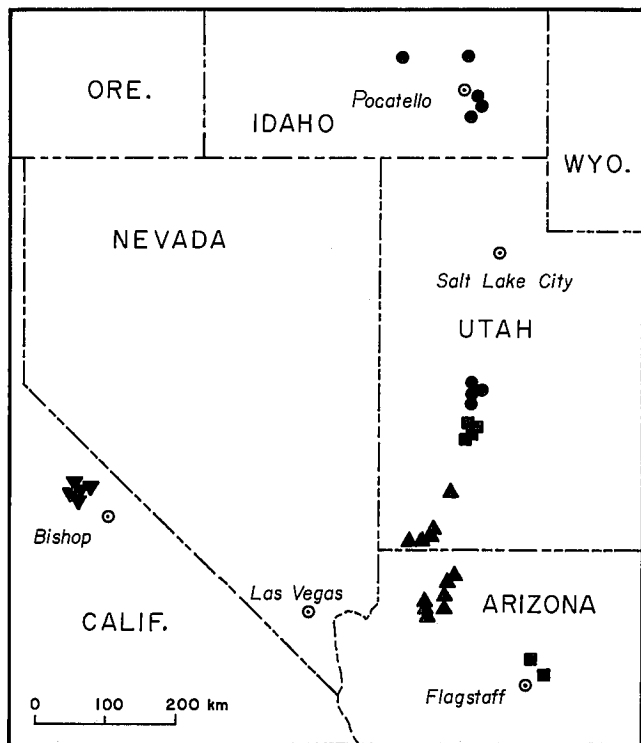


FIGURE 1. Index map of the western United States, showing the locations and geographic clustering of the TL samples. Symbols as in figure 4.

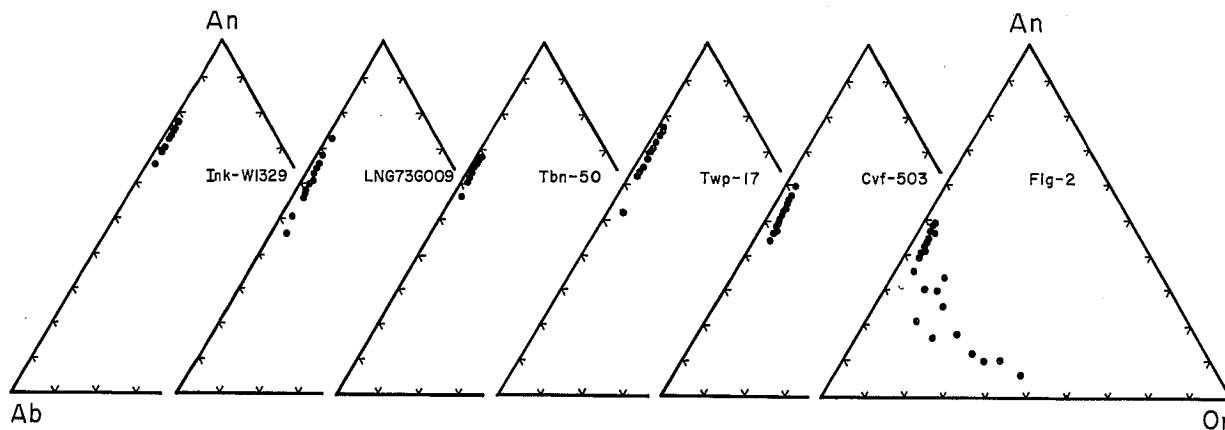


FIGURE 2. Microprobe analysis of feldspar compositions for selected samples.

^{235}U , ^{232}Th , and ^{40}K). U and Th concentrations were determined by gamma-ray spectrometry. K determinations were made by X-ray fluorescence spectrometry. Dose rates were calculated using the coefficients given by Bell (1976).

Radioelement Determinations

Gamma-ray spectrometry was used for the U and Th determinations. A NaI(Tl) scintillation detector enclosed in a shielding of powdered dunite was attached to a 256-channel multichannel analyzer. The resulting spectra were analyzed with the aid of a PDP-10 computer. Corrections were made for variations in background intensities, amplifier gain, and detector efficiency. Spectrum stripping was accomplished using the algorithms of Adams and Gasparini (1970, p. 156).

The 2.14 MeV and 1.76 MeV gamma emissions from ^{208}Tl and from ^{214}Bi , respectively, were used to measure the concentrations of Th and U, respectively; secular equilibrium was assumed. This assumption of secular equilibrium may not be

strictly valid for such young samples, and some of the determinations may be biased in this regard. However, the internal consistency of the results within the several geological suites and the absence of anomalous Th/U ratios, except for rocks of atypical composition, suggest that such systematic errors are small.

New Brunswick Laboratory Analyzed Samples No. 74 (1000 ppm U) and No. 80 (1010 ppm Th, 40 ppm U) (C. J. Rodden 1958 written comm. to W. H. Brimhall) were the primary standards used in this study. A sample of the Table Mountain Latite (Slemmons 1966) analyzed by gamma-ray spectrometry at Lawrence Berkeley Laboratories (A. R. Smith 1977 written comm.) was analyzed as a secondary standard. Other standard samples analyzed included the USGS Standard Rock QLO-γ (Walker and others 1976, Millard 1976), The Conway Granite, and the Conway Diabase (W. H. Brimhall 1977 pers. comm.). Table 2 compares the results of these determinations with the previously reported analyses of these samples. The discrepancies for sample QLO-γ probably represent inaccuracies in the U and Th determinations reported by Walker and others (1976), which were performed by the fluorometric and spectrophotometric methods, respectively (Stuckless and others 1976).

Six basaltic samples were analyzed by gamma-ray spectrometry at BYU and at Lawrence Berkeley Laboratories (Smith 1977 written comm.) and provide an important measure of interlaboratory variations and uncertainties for samples of such typically low radioelement contents. Table 3 compares the results of my determinations with the results reported by Smith. Statistical measures of the differences between the two sets of determinations show that they are in excellent agreement; the mean ratio of the Th values is 0.998 ($1\sigma = 0.062$), and the mean ratio of the U values is 0.998 ($1\sigma = 0.046$).

For results of the U and Th determinations for the basaltic samples used in the TL study, see table 4. Analytical precision for replicate analyses was generally equal to the counting statistics uncertainty; the counting statistics relative standard deviations (at the 2σ or 95% confidence level) range from 2 to 4% and were in no case larger than 6%. On the basis of the interlaboratory comparison and upon the analysis of the standard samples cited above, the U and Th determinations reported here are believed to be accurate to within approximately 5% relative.

The method of Norrish and Hutton (1969) was used to measure potassium contents by X-ray fluorescence spectrometry. Potassium determinations were made in conjunction with the whole-rock analyses reported in Appendix 2. Precision of the method is better than 1% relative, and accuracy, as indicated by the analysis of international rock standards, is better than 1.5% relative. The K_2O determinations for the basaltic samples used in the study are reported in table 4.

TABLE 1
MICROPROBE ANALYSIS OF PLAGIOCLASE SEPARATES

SAMPLE	AN ^{AVG*}	AN ^{RANGE*}	OR ^{AVG*}
LNG73G001	54	44-61	2.3
LNG73G008	61	55-63	2.0
LNG73G009B	59	47-73	2.2
LNG73G012	48	42-56	3.3
LNG73G014	52	45-71	2.8
LNG74G011	65	62-69	1.3
Ink-W1329	72	66-77	1.5
Ink-W1330	67	64-76	2.1
Mcc-W1121	61	49-69	1.9
Cmn-1	47	45-48	3.8
Nel 1-B	61	50-66	1.8
SG-81	62	59-65	2.8
Zion-68	54	46-61	2.6
Zion-69	63	60-65	2.2
SG-33B	59	55-63	1.3
Whw-2	58	46-66	2.0
Whw-6-3	58	48-65	1.8
Whw-9	62	58-66	1.7
Vulc-11	57	49-68	2.3
U49	71	69-73	1.6
Twp-17	69	63-77	1.8
Htn-18	67	65-69	1.2
Pav-51	57	36-72	2.7
Pav-53	63	55-72	1.7
Pav-54A	69	53-76	1.5
Brd-6	59	57-62	1.6
Tbn-50	64	60-70	1.6
Cov-51	51	30-60	2.9
Cov-54	48	38-58	3.3
Cov-55	57	50-63	2.7
Cvf-503	52	45-60	3.1

*As weight percent.

TABLE 2
INTERLABORATORY COMPARISON OF U AND TH DETERMINATIONS FOR STANDARD SAMPLES

SAMPLE	U (PPM)		Th (PPM)	
	BYU	OTHER	BYU	OTHER
Table Mt. Latite	11.01 ± 0.12	10.48 ± 0.06 ^a	32.18 ± 0.36	31.56 ± 0.20 ^a
QLO-γ	1.89 ± 0.05	1.58 ± 0.13 ^b 2.01 ± 0.10 ^c	5.28 ± 0.16	3.52 ± 0.63 ^b 3.24 ± 1.20 ^c
Conway Granite	14.99 ± 0.19	12.86 ± 0.33 ^d	52.84 ± 0.69	54.12 ± 0.97 ^d
Conway Diabase	22.82 ± 0.18	21.77 ± 0.57 ^d	7.83 ± 0.18	8.40 ± 0.15 ^d

^aSmith, A. R., 1977, written comm.

^bWalker, G. W., and others, 1976, p. 19.

^cMillard, H. T., Jr., 1976, p. 64.

^dBrimhall, W. H., 1977, pers. comm.

TABLE 3
INTERLABORATORY COMPARISON OF U AND Th DETERMINATIONS FOR BASALTIC SAMPLES

SAMPLE	U (PPM)		Th (PPM)	
	BYU	LBL ^a	BYU	LBL ^a
Cvf-503	1.35 ± 0.04	1.334 ± 0.015	5.85 ± 0.15	5.971 ± 0.049
Ice-51C	1.04 ± 0.03	1.033 ± 0.016	3.24 ± 0.12	3.325 ± 0.050
Ink-W1329A	0.49 ± 0.02	0.479 ± 0.005	1.64 ± 0.07	1.637 ± 0.14
LNG73G009B	1.15 ± 0.04	1.218 ± 0.011	4.54 ± 0.13	4.304 ± 0.035
Pav-54A	0.54 ± 0.02	0.525 ± 0.007	2.16 ± 0.09	1.976 ± 0.022
Tbn-50	0.52 ± 0.03	0.537 ± 0.007	1.91 ± 0.08	1.909 ± 0.022
Vulc-11	1.18 ± 0.03	1.263 ± 0.013	5.02 ± 0.14	5.603 ± 0.044

^aSmith, A. R., 1977 written comm.

Dose Rate Calculations

Dose rate calculations were made with the use of the coefficients given by Bell (1976); May (1975) has reviewed the background and theory of these calculations. Following Aitken and Bowman (1975; see also Aitken 1974, p. 100; and May 1975), I estimated the effectiveness of alpha particles in producing TL to be 0.10 (10%) of their nominal energy. This lower effectiveness in producing TL electrons is due to the fact that alpha particles expend their entire energy in a very short path (25 microns) and that all the available traps are filled by just a fraction of the ionized electrons; the remaining electrons return to the valence state and produce no TL signal. The cosmic-ray contribution to the dose rate was assumed to be constant and negligible (May 1975).

TABLE 4
U, Th, AND K₂O DETERMINATIONS

SAMPLE	U (PPM)	Th (PPM)	K ₂ O WT%
LNG73G001	1.10 ± 0.03	4.12 ± 0.13	2.23
LNG73G008	0.87 ± 0.03	3.53 ± 0.12	2.07
LNG73G009B	1.15 ± 0.04	4.54 ± 0.13	1.73
LNG73G012	1.00 ± 0.03	4.00 ± 0.15	2.24
LNG73G014	0.94 ± 0.03	3.28 ± 0.11	1.83
LNG74G011	0.66 ± 0.03	2.40 ± 0.09	1.06
Flg-1	3.58 ± 0.06	11.04 ± 0.19	2.48
Flg-2	3.72 ± 0.06	11.50 ± 0.22	2.56
Ink-W1329	0.49 ± 0.02	1.64 ± 0.07	1.11
Ink-W1330	0.45 ± 0.02	1.55 ± 0.07	0.96
Mcc-W1121	0.37 ± 0.02	1.49 ± 0.07	0.59
Cmn-1	2.01 ± 0.05	6.80 ± 0.17	1.87
Nel 1-B	0.43 ± 0.02	1.63 ± 0.08	0.80
SG-81	1.55 ± 0.04	5.98 ± 0.14	1.35
Zion-20	1.22 ± 0.03	4.00 ± 0.15	2.41
Zion-68	1.20 ± 0.04	4.83 ± 0.14	1.07
Zion-69	0.75 ± 0.03	2.91 ± 0.11	1.93
SG-33B	0.41 ± 0.02	1.39 ± 0.07	0.62
Whw-2	1.66 ± 0.04	5.94 ± 0.15	1.38
Whw-6-3	1.69 ± 0.04	6.36 ± 0.10	0.96
Whw-9	1.32 ± 0.04	4.74 ± 0.13	1.11
Vulc-11	1.18 ± 0.03	5.02 ± 0.14	0.84
U49	1.76 ± 0.04	5.02 ± 0.14	1.42
Twp-17	1.62 ± 0.04	6.08 ± 0.16	1.68
Htm-18	1.78 ± 0.04	6.96 ± 0.16	0.83
Pav-51	0.54 ± 0.02	1.96 ± 0.09	1.07
Pav-53	0.48 ± 0.02	2.20 ± 0.09	1.11
Pav-54A	0.54 ± 0.02	2.16 ± 0.09	1.17
Brd-6	0.75 ± 0.03	3.28 ± 0.13	1.17
Tbn-50	0.52 ± 0.03	1.91 ± 0.08	0.98
Cov-51	1.40 ± 0.04	5.66 ± 0.15	2.23
Cov-54	1.43 ± 0.04	5.87 ± 0.15	2.24
Cov-55	1.45 ± 0.04	8.81 ± 0.19	3.16
Cvf-503	1.35 ± 0.04	5.85 ± 0.15	2.33

The whole-rock dose rates were calculated from the radioelement concentrations in table 5 according to the formula:

$$r_{\text{rock}} = a(\text{U ppm}) + b(\text{Th ppm}) + c(\text{K}_2\text{O wt.}\%) \quad (\text{Eq. 1}),$$

where a, b, and c are the coefficients of Bell and have the units of rads/yr per ppm or rads/yr per weight percent. They are given in table 5. Their relative standard deviations were calculated according to the formula:

$$\epsilon^2_{\text{rock}} = (\epsilon^2_{\text{U}} + \epsilon^2_{\text{Th}} + \epsilon^2_{\text{K}_2\text{O}}) \quad (\text{Eq. 2}).$$

$\epsilon^2_{\text{K}_2\text{O}}$ was assumed to be 2% for the purpose of this calculation.

Because a larger portion of its total decay energy is likely to be absorbed by the dosimeter crystal, potassium incorporated into the plagioclase solid solution series makes a relatively larger contribution to the sample dose rate than does potassium scattered throughout the other mineral phases of the rock. The "composite" dose rates reported in table 5 were calculated in order to allow for this difference in relative efficiency. The potassium contents of the plagioclase samples were determined by electron microprobe analysis; they are reported in table 1 as weight percent orthoclase. Although U and Th produce more than half the whole-rock dose rate, their contribution to the plagioclase internal dose rate was assumed to be negligible for two reasons: (1) U and Th are preferentially incorporated into other mineral phases as the basaltic melts crystallize, and (2) no analytical determinations of U and Th in the plagioclase separates were available. Composite dose rates were calculated according to the formula:

$$r_{\text{composite}} = 0.75(r_{\text{rock}}) + 1.5(r_{\text{plag}}) \quad (\text{Eq. 3}),$$

where r_{plag} , the plagioclase internal dose rate, represents the dose rate produced by potassium in the plagioclase crystals and is calculated according to the formula:

$$r_{\text{plag}} = \text{Or}(0.169 \text{ wt}\% \text{ K}_2\text{O}/\text{wt}\% \text{ Or}) \times (0.0887 \text{ rads/y wt}\% \text{ K}_2\text{O}) \quad (\text{Eq. 4}).$$

The plagioclase dose rate, on the average, is $17.3 \pm 6.0\%$ of the whole rock dose rate. The factor of 1.5 in the composite dose rate equation (Eq. 3) was chosen in order to give the average plagioclase portion of the composite dose rate a weight equivalent to 25% of the total dose rate. This proportion was empirically chosen in order to give the best possible results for sample Mcc-W1121 which exhibits a noticeably low overall dose rate relative to its TL intensity. The relative standard deviation of the composite dose rate is given by:

$$\epsilon^2_{\text{composite}} = \epsilon^2_{\text{rock}} + \epsilon^2_{\text{plag}} \quad (\text{Eq. 5}).$$

A relative standard deviation of 7.8% was assumed for ϵ_{plag} . In most cases the true deviance is somewhat higher; however, the plagioclase contribution to the composite dose rate averages only 25% of the total dose rate, and the selected value of 7.8% effectively weights this uncertainty so that it is approximately equal to the whole-rock dose rate uncertainty. In any case, the TL uncertainties are much larger than the dose rate uncertainties; therefore, small errors in the calculation of the dose rate uncertainties have an inconsequential effect on the final TL calculations.

Whole-rock dose rates do not take into consideration the spatial distribution of radioelements relative to the size and location of the dosimeter crystals. For this reason, the composite dose rates were judged to more accurately reflect the "true" dose rates received by the plagioclase samples. The composite dose rates were used for all TL calculations; in most cases, the composite dose rates are not significantly different from the whole-rock dose rates (see table 5).

TL MEASUREMENTS

The equipment of the U.S. Geological Survey laboratories at Menlo Park, California, was used to make thermoluminescence measurements. Dalrymple and Doell (1970) and May (1975, 1977) have described in detail the equipment and techniques used. An SSR model 1105/1120 photon counter/amplifier-discriminator was used. A Corning CS-560 blue filter was used to filter the TL emission measured by an EMI 9635 photomultiplier tube. The maximum spectral sensitivity of this system occurs at 380–420 nm, the wavelength of blue light. Unfortunately, the photon counter and photo-

multiplier units used during this study were not the same units used by May in his study of the TL dating of Hawaiian basalts, and, therefore, it is not possible to compare our results directly. Artificial TL was induced by a standard 96-second exposure to the beam of a W-target X-ray tube; this dose is equivalent to ~1600 roentgens.

Natural and artificial TL glow curves typical of the samples used in this study are shown in figure 3. To a first approximation, these glow curves are identical to those previously reported for natural plagioclase crystals (see May 1975, Dalrymple and Doell 1970, Berry 1973, Hwang 1971, and Geake and others 1973). However, a closer examination suggests that there are two distinct types of glow curves produced by the samples used in this study. The distinguishing criterion is the shape of the glow curve as revealed by the resolution and relative magnitude of the 325° C artificial TL peak. In Type I glow curves the peak at 300–350° C is clearly resolved and dominates the portion of the glow curve above 200° C. In contrast, the Type II glow curves do not have a clearly defined high-temperature peak; the dominant low-temperature peak drops off rapidly, and there is no noticeable high-temperature peak. Moreover, the absolute level of the high-temperature TL emission is generally lower than that of the Type I samples (see table 6). This finding is significant because it indicates that the high-temperature peak is not merely being obscured by unusually intense peaks at lower temperatures, but rather that it is either absent or is significantly attenuated in these samples. Although there are general trends of petrochemical similarity between the samples exhibiting each type of glow-curve morphology, the parameter controlling this feature is still unknown.

In his study of the TL of Hawaiian basalts, May (1975, p. 70) encountered similar problems regarding the inadequate resolution of the high-temperature artificial TL peak. By allowing his samples to decay at room temperature for 10 to 40 days after irradiation, he was able to significantly improve the resolution of the high-temperature artificial TL peak since the low-temperature peaks decay more rapidly at room temperature. He routinely uses a technique of 60-day delays for the TL dating of sanidines in silicic volcanics (pers. comm. 1977). Insufficient time was available in this study to use such techniques to improve the resolution of these artificial TL peaks. Moreover, in a series of artificial TL measurements conducted after a 7-day delay, for 6 samples, including one Type I sample, there was no significant improvement in the resolution of the high-temperature peak even though the overall levels of TL intensity were reduced by a factor of 2–4. This lack of improvement lends further support to the hypothesis that this high-temperature artificial TL peak is either absent or strongly attenuated in the Type II samples.

This contrast in the resolution and magnitude of the high-temperature peak between the Type I and Type II samples suggested that it would be necessary to treat these samples separately in the construction of the TL vs. age calibration curves. Accordingly, the samples were separated into two groups, Type I and Type II, on the basis of glow-curve morphologies and magnitudes. The Type III samples (see below) exhibit Type II glow-curve morphologies. Several samples exhibited glow-curve shapes appropriate to a given type but had TL intensities, either natural or artificial, that varied erratically from 5 to 100 times less than the intensities typical of that group or were, in one case (U49), over 20 times more intense than the typical values. Such samples were judged to be anomalous and were not included in later calibrations of TL vs. age if they were of known age, or were not dated by the TL method if they were

TABLE 5
DOSE RATE CALCULATIONS

SAMPLE	t_{rock}^*	ϵ_{rock}	t_{plag}^*	ϵ_{comp}^*	ϵ_{comp}
LNG73G001	0.322	4.85%	0.035	0.297	9.2%
LNG73G008	0.286	5.09	0.030	0.260	9.3
LNG73G009B	0.286	4.92	0.034	0.266	9.2
LNG73G012	0.315	5.31	0.049	0.314	9.4
LNG73G014	0.264	5.02	0.042	0.261	9.3
LNG74G011	0.167	5.86	0.020	0.155	9.8
Flg-1	0.587	3.08	0.131	0.637	8.4
Flg-2	0.608	3.24	0.169	0.710	8.4
Ink-W1329	0.151	6.47	0.023	0.148	10.2
Ink-W1330	0.134	6.73	0.031	0.147	10.3
Mcc-W1121	0.096	7.32	0.028	0.114	10.7
Cmn-1	0.381	3.97	0.058	0.373	8.8
Nel 1-B	0.120	7.21	0.027	0.131	10.6
SG-81	0.297	3.88	0.043	0.287	8.7
Zion-20	0.342	5.10	0.189	0.540	9.3
Zion-68	0.235	4.68	0.038	0.233	9.1
Zion-69	0.257	5.59	0.032	0.241	9.6
SG-33B	0.099	6.94	0.020	0.104	10.4
Whw-2	0.305	4.04	0.030	0.274	8.8
Whw-6-3	0.276	4.13	0.027	0.248	8.8
Whw-9	0.244	4.35	0.026	0.222	9.0
Vulc-11	0.216	4.46	0.035	0.215	9.0
U49	0.321	4.11	0.024	0.277	8.8
Twp-17	0.331	4.29	0.027	0.289	8.9
Htn-18	0.278	3.87	0.018	0.236	8.7
Pav-51	0.155	6.70	0.041	0.178	10.3
Pav-53	0.159	6.38	0.026	0.158	10.1
Pav-54A	0.167	6.43	0.022	0.158	10.1
Brd-6	0.195	6.02	0.023	0.181	9.8
Tbn-50	0.145	7.41	0.024	0.145	10.8
Cov-51	0.362	4.32	0.044	0.338	8.9
Cov-54	0.367	4.31	0.051	0.352	8.9
Cov-55	0.495	3.95	0.041	0.433	8.8
Cvf-503	0.362	4.32	0.047	0.342	8.9

*In rads/year.

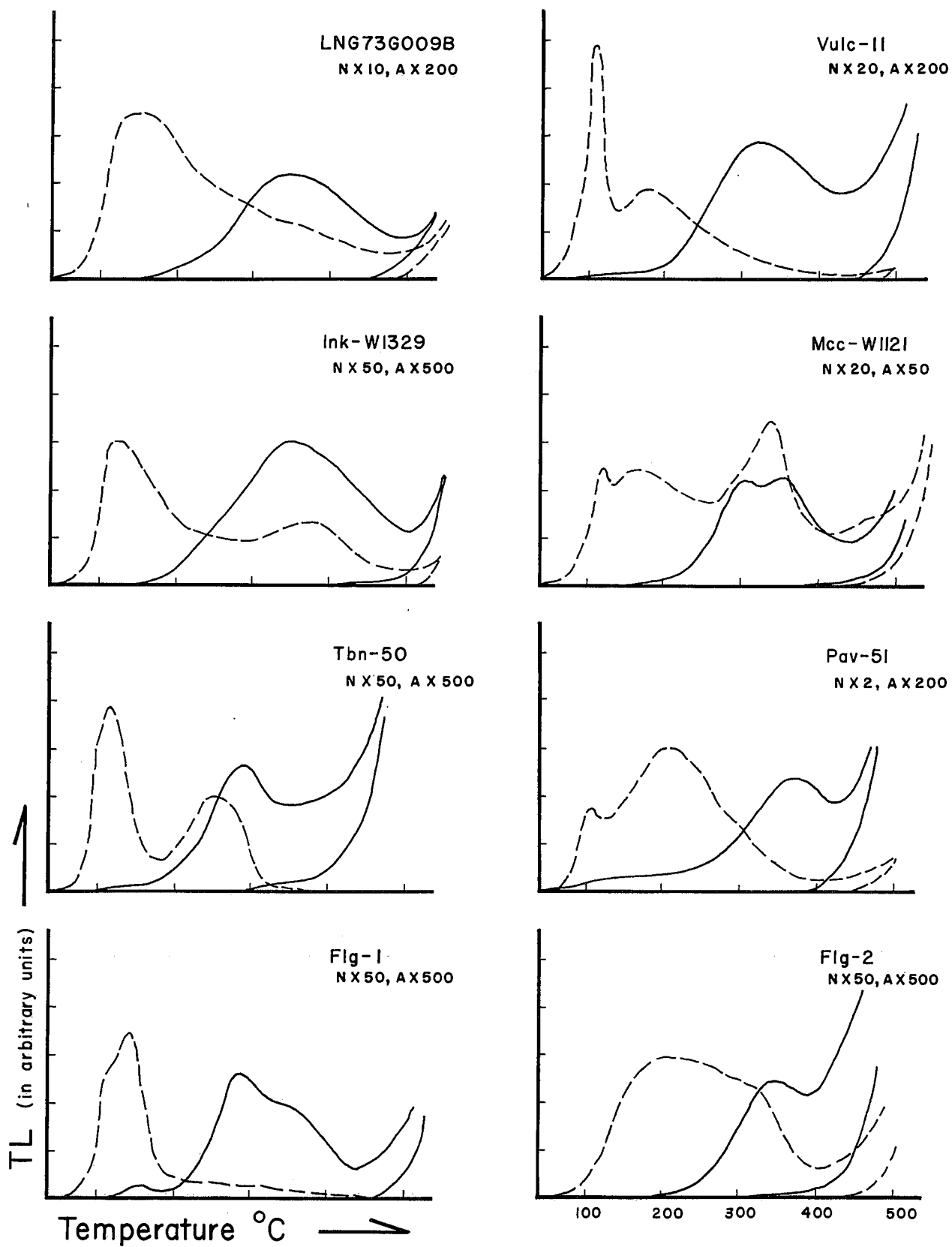


FIGURE 3. Typical TL glow curves for selected samples. Natural TL signals are shown by solid lines, artificial TL signals by dashed lines; appropriate scale factors are shown for each sample.

of unknown age. Eleven samples were rejected according to this criterion (LNG73G001, LNG73G012, Flg-1, Flg-2, Zion-20, Nel 1-B, SG-33B, U49, Pav-51, Pav-53, Pav-54A).

The erratic and anomalous nature of the TL response of some samples is vividly demonstrated by the contrasting glow-curve morphologies of two petrologically and geographically related samples, Tbn-50 and Pav-51, as shown in figure 3. In only three cases can these TL anomalies be unquestionably correlated to impure separations (Flg-1, Flg-2, Zion-20). Such anomalous results in samples with demonstrably clean separates (e.g., Pav-53, Pav-54A and Nel 1-B) are unexplained. May (1977) observed an anomalously high artificial TL level in the plagioclase separates of one of his alkalic Hawaiian basalts but did not speculate on its cause. Wintle (1973) observed "anomalous fading" of the natural TL in feldspar samples younger than 50,000 years; he did not suggest a mechanism to explain these losses. Such irregularities in the acquisition and retention of TL emphasize the subtle nature of the factors which affect the TL behavior of a sample.

The results of the TL measurements on samples not exhibiting anomalous glow-curve morphologies or intensities are given in table 6. In all cases, the average ratio N/A for the measured replicates (a minimum of seven) was calculated by the method which gave the smallest uncertainty; i.e., either the ratio of the averages, the average of the ratios, or some weighted average thereof was used. The TL ranges cited exclude any anomalous replicates.

SPECIFIC TL CALCULATIONS AND TL AGE DATING

In the development of a relative TL age-dating scheme, it is necessary to construct calibration curves relating TL intensity to age for samples of known age. Such a calibration curve can then be used to calculate the age of unknown samples based upon their TL intensities. Such a method alleviates many of the uncertainties inherent in the calculation of "absolute" ages from the raw TL data. However, in making such a calibration it is necessary that all the samples be of the same rock type and have similar TL characteristics.

Petrochemical Variations

The samples used in this study form six distinct geographic and petrochemical groups: (1) high-alumina basalts from the Long Valley Caldera, California; (2) olivine tholeiites from the Snake River Plain, Idaho; (3) olivine tholeiites from the Black Rock Desert, Utah; (4) alkalic basalts from southern Utah and northern Arizona; (5) basaltic andesites from the San Francisco volcanic field, Arizona, and (6) basaltic andesites from the Cove Fort field, Utah. Each group exhibits a slightly different type of TL response and, strictly speaking, should be grouped and analyzed separately. However, the effects of variations and similarities in bulk petrochemistry seem to dominate over those of "geography," with the result that basalts of roughly similar composition can be grouped together to construct relative dating curves. Such grouping reduces the number of distinct groups to three: (1) Type I samples, the olivine tholeiites from Idaho and the Black Rock Desert, Utah; (2) Type II samples, the alkalic basalts of southern Utah, northern Arizona, and Long Valley; and (3) Type III samples, the basaltic andesites of the Cove Fort and San Francisco volcanic fields. Such a division of TL samples on the basis of petrochemical differences is not new; May (1975) segregated his Hawaiian basalts into two groups, tholeiitic and alkalic basalts.

Three criteria were used to group the samples into the three "types" introduced above: (1) geographic locality, (2) petrochemical similarities and differences, and (3) variations in glow-curve morphology. The geographic clustering of the samples is illustrated in figure 2. The discrimination of the two distinct types of glow curves was discussed in the preceding section. Variations in petrochemistry and the correlation of specific TL ratio to age will be discussed below.

The petrochemical similarities and differences between the different sample types are illustrated in the variation diagrams shown in figures 4, 5, and 6. Chemical analyses and CIPW norms for each sample are given in the appendix. A brief petrographic description of each sample may be obtained from the author.

The basalts of Type I are olivine tholeiites in the normative classification of Yoder and Tilley (1962). They are characterized

TABLE 6
TL MEASUREMENTS

SAMPLE	NAT. TL RANGE*	ART. TL RANGE*	N/A	ϵ_{TL}	TYPE
LNG73G008	50-80	100-150	0.532	27%	II
LNG73G009B	20-50	70-120	0.324	20	II
LNG73G014	10-15	90-105	0.133	12	II
LNG74G011	20-50	30-60	0.565	19	II
Ink-W1329	70-100	260-360	0.314	24	I
Ink-W1330	45-75	200-350	0.225	20	I
Mcc-W1121	15-30	80-90	0.297	25	I
Cmn-1	145-180	400-550	0.355	10	I
SG-81	165-300	165-180	1.852	25	II
Zion-68	19-33	14-20	1.563	15	II
Zion-69	400-1000	40-360	3.846	48	II
Whw-2	55-80	230-330	0.243	15	II
Whw-6.3	90-110	80-125	0.917	8	II
Whw-9	15-70	80-115	0.282	25	II
Vulc-11	25-65	30-60	0.781	15	II
Twp-17	19-29	10-18	1.887	15	II
Htn-18	35-50	18-35	1.667	23	II
Brd-6	40-65	20-33	1.220	26	I
Tbn-50	60-105	465-635	0.144	12	I
Cov-51	510-600	160-210	3.226	4	III
Cov-54	310-360	115-150	2.513	5	III
Cov-55	49-75	47-58	1.099	16	III
Cvf-503	130-160	70-110	1.408	6	III

*In arbitrary units.

by low alkalis, high iron content, and a distinctly tholeiitic trend on the AFM diagram. The two samples that differ noticeably from the rest of the group are Cmn-1, an "evolved" tholeiite from the Craters of the Moon field (Leeman and others 1976), and Brd-6, a sideromelane-palagonite tuff from Pavant Butte in the Black Rock Desert (Hoover 1974).

As evidenced by their trends on the alkalis vs. silica variation diagram and on the AFM diagram, the Type II basalts are distinctly alkaline. The Long Valley samples, Type II-A, are high-alumina basalts and andesites with 4–7% total alkalis ($\text{Na}_2\text{O} + \text{K}_2\text{O}$). They appear to be very similar, chemically, to the "alkali-rich high-alumina basalts" described by Moore and others (1976) from the San Francisco volcanic field. The Type II-B samples from Utah and northern Arizona, in contrast, have lower contents of alumina and total alkalis. They are nor-

matively classed as hawaiites, alkali olivine basalts, and basanites. Their petrochemical characteristics and distribution have been discussed by Best and Brimhall (1974). In spite of the differences between the Type II-A and II-B basalts, they are grouped together as one TL suite because (1) their petrochemical differences are small compared to their differences relative to Type I or Type III basaltic rocks, (2) the morphology of their glow curves is very similar, (3) they have similar dose rates, and (4) their specific TL ratios vs. age plot on the same line for the available samples of known age.

The Type III samples include basaltic andesites from the Cove Fort field (Clark 1977) and from the San Francisco volcanic field (Moore and others 1976). These samples exhibit somewhat calc-alkaline petrochemical trends. They are sub-alkaline on the alkalis vs. silica variation diagram; their trend on the AFM diagram is nearly calc-alkaline; and, on a plot of alumina vs. normative plagioclase composition (Irvine and Baragar 1971), they are marginally calc-alkaline. The samples from the Cove Fort field are noticeably more calc-alkaline than those from the San Francisco volcanic field. The two basaltic andesites from the San Francisco field were both rejected for TL dating because of impure separations and anomalous glow-curve morphologies.

Specific TL Ratio Calculations

Specific TL, R , is a measure of the relative proportion of the available electron traps that are filled after correcting for intersample variations in the dose rate. It is calculated according to the formula (May 1975, p. 119; see also Aitken 1974, p. 86):

$$R = 100 y^{-1} \left(\frac{N}{A} \right) \left(\frac{D}{r} \right) \quad (\text{Eq. 6}),$$

where N/A is the ratio of natural TL intensity to the artificial TL intensity produced by a dose of D rads; r is the dose rate in rads per year.* The constant $100 y^{-1}$ is required to make the

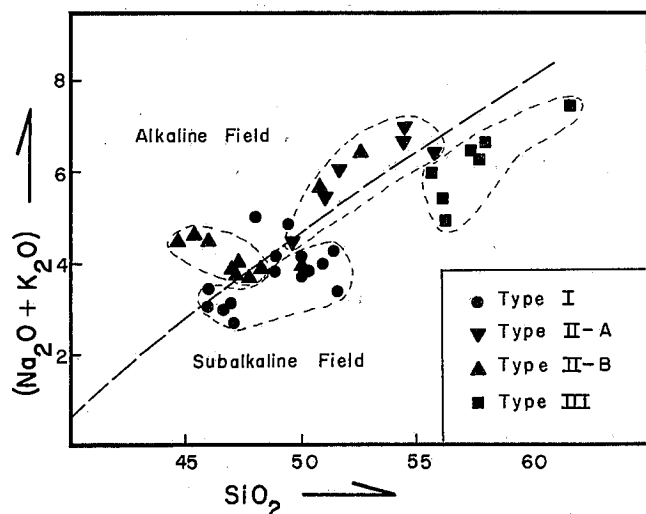


FIGURE 4. Alkalies vs. silica variation diagram showing alkaline nature of Type II samples. Dividing line is after Irvine and Baragar (1971).

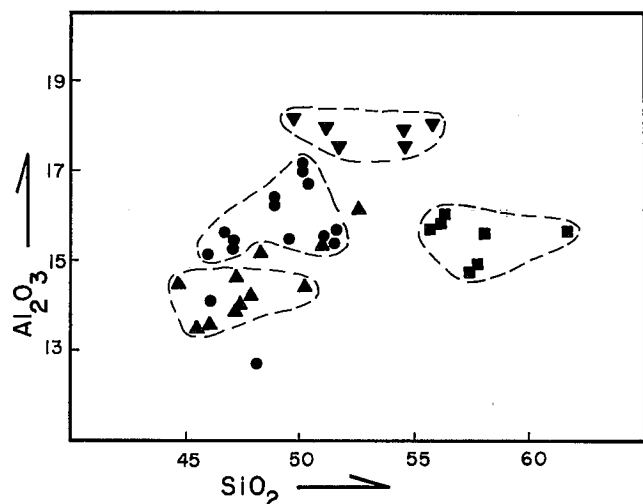


FIGURE 5.—Alumina vs. silica variation diagram showing high alumina content of Long Valley Caldera samples (Type II-A). Symbols as in figure 4.

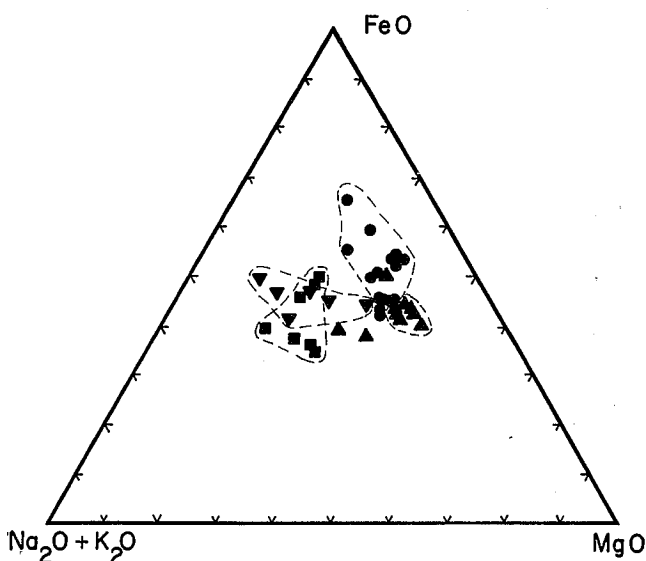


FIGURE 6.—AFM variation diagram illustrating tholeiitic trend of Type I samples. Symbols as in figure 4.

*The artificial dose, D , was assigned a value of 1.0 because (1) it is constant for all samples and because (2) the appropriate conversion factor from roentgens to rads is unknown for plagioclase (May 1977 pers. comm.).

specific TL ratio a dimensionless number and to insure that $\log(R)$ is positive. The composite dose rate calculated above is used for all specific TL ratio calculations in this section. Table 7 presents the specific TL and its uncertainty calculated for each sample. By plotting these values against age for the samples of known age it is possible to construct the TL calibration curves given in figures 7 and 8.

The Type I samples of known age range from 2,000 to 33,000 years and fit the calibration line best when plotted on a semilogarithmic base (fig. 7). The equation of the best-fit line connecting the five Type I samples is:

$$\log(R) = 1.4469 \times 10^{-5}(\text{age}) + 1.8841 \quad (\text{Eq. 7}),$$

$$(r^2 = 0.931)$$

where r^2 is the correlation coefficient. For the purpose of constructing the best-fit calibration line the sample Tbn-50 was assigned a tentative age of $10,000 \pm 3,000$ years. Hoover (1974) estimates that the Tabernacle flow is less than 12,000 years old on the basis of the absence of Lake Bonneville erosional terraces. The sample Cmn-1 has a noticeably high TL level; there is a strong possibility that this sample does not correspond to the dated standard and was inaccurately collected (Kowallis pers. comm. 1977). May (1975, p. 115) observed anomalously high TL intensities in very young tholeiitic basalts; the high TL intensities of Cmn-1 may be a similar phenomenon. Because sample Cmn-1 deviates significantly from the trend established by the samples of known age in the 25,000 to 33,000 y. range, the sample Tbn-50 was assigned a weight of 2 in order

to reduce the effective weight of Cmn-1 in calculating the regression. Sample Brd-6 yields the oldest TL age for any Type I sample; it is considerably older than any of the samples of known age in this class, and, therefore, its TL age is somewhat more uncertain. Its projected position and age uncertainty are shown in figure 7 to illustrate this uncertainty.

In contrast to the Type I samples, the best-fit calibration for the Type II samples plots on a log-log base. The samples of known age range from 62,000 to 440,000 years old and come from two geographic areas, the Long Valley Caldera and south-ern Utah. The best-fit equation is:

$$\log(R) = 1.695 \log(\text{age}) - 6.430 \quad (\text{Eq. 8}).$$

$$(r^2 = 0.981)$$

It is noteworthy that plotted on a linear base, the Long Valley samples form a nearly perfect linear relation. The best-fit linear equation is:

$$R = 1.860 \times 10^{-3}(\text{age}) - 66.75 \quad (\text{Eq. 9}).$$

$$(r^2 = 0.9994)$$

However, this linear calibration produces poor results for the two older Type II samples from Utah. The log-log calibration appears to be the best overall fit. The TL ages of the unknown Type II samples were calculated using this calibration (Eq. 14) and are reported in table 7.

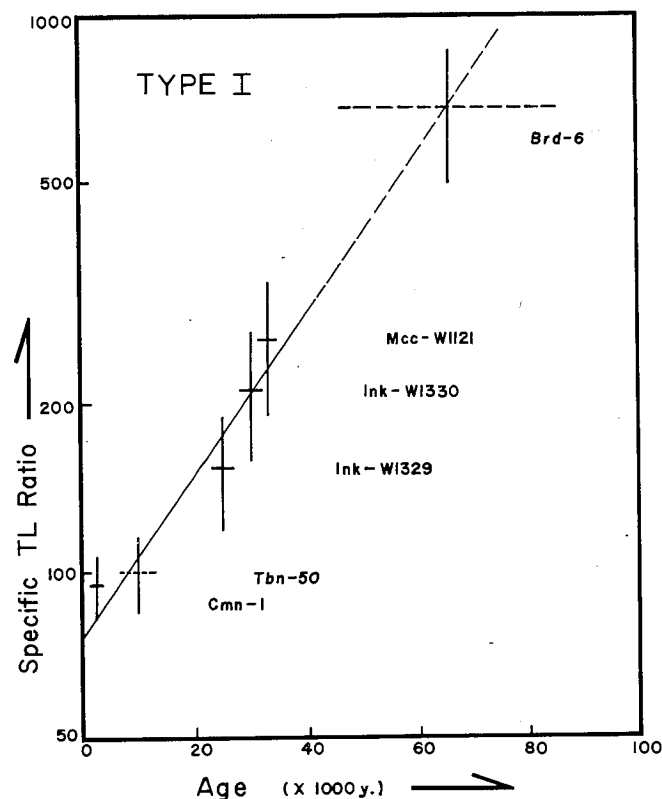


FIGURE 7.—Semilogarithmic plot of specific TL ratio, R , vs. age for Type I samples (olivine tholeiites). Samples Tbn-50 and Brd-6 are not radiometrically dated calibration points but are included to show their relationship to samples of known age.

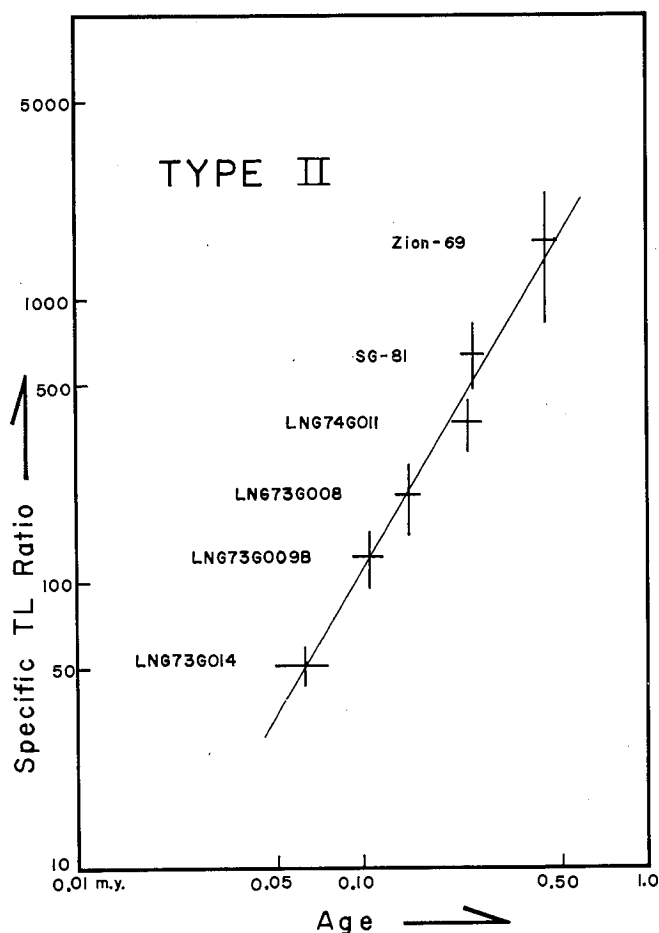


FIGURE 8.—Log-log plot of specific TL ratio, R , vs. age for Type II samples (alkalic basalts) of known age.

Aside from the Flagstaff samples, which had impure plagioclase separates, there are no Type III samples which have age dates with low uncertainties. M. G. Best (1978 pers. comm.) has obtained preliminary K-Ar dates for two samples equivalent to Cvf-503 and to Cov-55. They are 0.5 ± 0.1 m.y. and 0.3 ± 0.1 m.y., respectively. This shows a general trend of increasing TL with age, but the exact calibration remains uncertain. Moreover, extension of this trend yields geologically unreasonable ages for samples Cov-51 and Cov-54. Since Cvf-503, Cov-51, and Cov-54 are all samples from the same series of flows, the basaltic andesites of the Cove Fort field (Clark 1977), it was decided to average their TL response and to assign this average value to the radiometrically determined age of 0.5 m.y. This averaged value and the TL response of the younger latite, Cov-55, produced a trend of increasing TL with age which is very similar to that of the Type II samples. However, because of the uncertainties of the TL data and of the K-Ar ages of the Type III samples, no attempt was made to date Type III samples of unknown age.

Discussion of the TL Results

The general form and trend of these TL vs. age calibrations offer important information on the uniformity and applicability of the TL age-dating technique. While these results clearly demonstrate that each suite of samples must be treated separately, they also demonstrate that there are certain broad similarities between groups. Figure 9, on a log-log base, shows the trend and extent of the specific TL data for each of the three sample types discussed above. The Type I trend represents only the three samples, Ink-W1329, Ink-W1330, and Mcc-W1121, which are judged to have the smallest TL and radiometric age date uncertainties and which exhibit the smallest variation in petrochemistry. The most striking feature of this graph is that all three trends have nearly the same slope. It suggests that, in spite of obvious differences between suites, there are important and fundamental similarities in the processes by which TL is acquired and stored over periods of geologic time.

Other investigators have reported the relationship of specific TL ratio to age to be either semilogarithmic (May 1975,

1977) or linear (Berry 1973). Indeed, a preliminary consideration of the simplest models of TL acquisition suggests that this relationship should be linear; i.e., since the dose rate is effectively constant and since the trapping probabilities and frequency factors should remain constant, the number of trapped electrons should simply be proportional to the age of the sample. This type of linear increase in TL is generally observed in measurements of artificial TL as a function of increasing radiation dose (May 1975, Berry 1973, Hwang and Goksu 1971, Dalrymple and Doell 1970). A linear acquisition of TL is also generally observed in the age dating of archaeological materials less than 10,000 years old.

The TL behavior of geological materials over long periods of time may be considerably more complex than this simple linear relation. May (1975, p. 115) reported a steady decrease in the artificial TL intensity of tholeiitic samples less than 30,000 years old. He attributed this to the "spontaneous annealing" of traps after the extrusion and cooling of the lavas. Samples older than this showed an increase in the artificial TL intensity, which May interpreted to indicate an increase in the number of available electron traps. He suggested that these additional traps were produced by the interaction with the plagioclase of alpha particles from the decay of radioelement impurities within the crystals. A similar trend of increasing artificial TL intensities was observed in alkalic basalts of all ages, and May (p. 121) proposed that specific TL increased exponentially with age in these samples. He proposed an equation of the form:

$$R = ae^{bt} \quad (\text{Eq. 10})$$

to describe the process, where b is approximately 1×10^{-5} and a is approximately 2.7. This relationship accurately describes the observed TL for seven of the eight alkalic basalts studied. May explained the exponential increase by suggesting that "the increase in trap density with age produces an even greater increase in the natural TL storage capacity . . . possibly by an increased initial trapping probability for conduction band electrons in samples with progressively larger trap densities" (1975, p. 123-24).

The data obtained in this study strongly suggest that this model of exponential increase in specific TL with age may not

TABLE 7
SPECIFIC TL RATIO CALCULATIONS

SAMPLE	R	ϵ_{Total}	TYPE	TL AGE	KNOWN AGE
LNG73G008	205 \pm 59	29%	II	143,000 \pm 42,000y.	145,000 \pm 15,000y
LNG73G009B	122 \pm 27	22	II	106,000 \pm 23,000	104,000 \pm 11,000
LNG73G014	51 \pm 8	15	II	63,000 \pm 9,500	62,000 \pm 13,000
LNG74G011	365 \pm 77	21	II	202,000 \pm 42,000	232,000 \pm 28,000
Ink-W1329	212 \pm 55	26	I	30,500 \pm 7,900	30,000 \pm 2,000
Ink-W1330	153 \pm 35	23	I	20,400 \pm 4,700	25,000 \pm 2,000
Mcc-W1121	260 \pm 70	27	I	36,800 \pm 9,900	33,000 \pm 1,600
Cmn-1	95 \pm 12	13	I	5,600 \pm 700	2,225 \pm 60
SG-81	645 \pm 168	26	II	282,000 \pm 73,000	244,000 \pm 21,000
Zion-68	671 \pm 121	18	II	289,000 \pm 52,000	
Zion-69	1596 \pm 782	49	II	481,000 \pm 236,000	440,000 \pm 40,000
Whw-2	89 \pm 15	17	II	88,000 \pm 15,000	
Whw-6-3	370 \pm 44	12	II	203,000 \pm 24,000	
Whw-9	127 \pm 34	12	II	108,000 \pm 29,000	
Vulc-11	363 \pm 62	17	II	201,000 \pm 34,000	
Twp-17	653 \pm 111	17	II	284,000 \pm 48,000	
Htn-18	706 \pm 177	25	II	297,000 \pm 74,000	
Brd-6	674 \pm 189	28	I	66,000 \pm 19,000	
Tbn-50	100 \pm 16	16	I	7,000 \pm 1,100	
Cov-51	954 \pm 95	10	III		
Cov-54	714 \pm 71	10	III		
Cov-55	254 \pm 46	18	III		
Cvf-503	412 \pm 45	11	III		

be accurate. The log-log correlations described above (see figs. 8 and 9) can be expressed as an equation of the form:

$$R = a(\text{age})^b \quad (\text{Eq. 11}),$$

where b has a value of approximately 1.7 and the intercept-value a varies from suite to suite. Such a function suggests somewhat different constraints for modelling and describing the mechanisms of TL acquisition and retention than those implied by an exponential model.

Since it is unlikely that specific TL can continue to increase at high rates indefinitely, I propose that the TL vs. age function might have the general shape shown in figure 10. TL increases linearly for young samples ($<10,000$ y.) to a point at which the number of additional defects produced by decay particles within the crystal significantly increases the TL storage capacity of the sample. At this point the number of trapped electrons begins to increase at a rate more rapid than that of the steady linear production of new traps. No mechanism to explain this supralinearity is proposed here. As the number of defects becomes large, a point of saturation may be reached. May (1975, p. 125) states: "Saturation is probably manifested initially by a decrease in the rate of accumulation of defects . . . this is probably due mainly to spontaneous annealing [of defects]." As equilibrium is reached between the processes producing and annealing the traps, the TL ratio should stabilize at

some plateau value which would then typify "older" samples (~ 1 m.y.). Such saturation effects were reported by May for samples 1.5 and 3.3 m.y. old; no evidence of saturation was found in the samples used in this study, all of which were less than 0.5 m.y. old.

Not enough experimental evidence now exists to definitively describe the processes acting in the acquisition, retention, and draining of natural TL signals. At this point, it is not possible to unequivocally select the "correct" model to describe this phenomenon. Future studies involving more numerous samples with better chemical, mineralogical, and age or stratigraphic control will be needed to more accurately describe the operation of the TL phenomenon as it acts in naturally occurring dosimeter crystals over geologically long periods of time.

SUMMARY AND CONCLUSIONS

Thirty-six samples were studied in order to develop a TL age dating technique for young continental basalts; 17 of the samples were of known age and served as calibration standards. Microprobe analysis of the plagioclase separates demonstrated that 33 were effectively pure plagioclase. Compositionally the separates ranged from oligoclase to bytownite; variations in plagioclase composition did not significantly affect the TL response of the samples.

The samples were divided into three groups or types on the basis of petrochemical, geographic, and TL similarities; the shape of the artificial TL glow curve was shown to be of primary importance for the accurate classification of the samples. TL calculations were made using a composite dose rate derived in order to compensate for variations in the amount of K_2O present in solid solution in the plagioclase dosimeter crystals. Calculations of the specific TL ratios showed that TL increased regularly in all three suites. The Type I samples showed the best correlation of specific TL to age when plotted on a semi-logarithmic base, whereas the Type II and Type III samples showed their best correlations when plotted on a log-log base. Significantly, a log-log plot of TL vs. age of selected samples from all three groups showed nearly identical slopes for each suite. This suggests that there are important similarities in the TL processes acting in each of the suites studied. TL ages were calculated for 10 Utah basalts of unknown age.

The data accumulated in this study lead to conclusions which require further investigation and confirmation by other

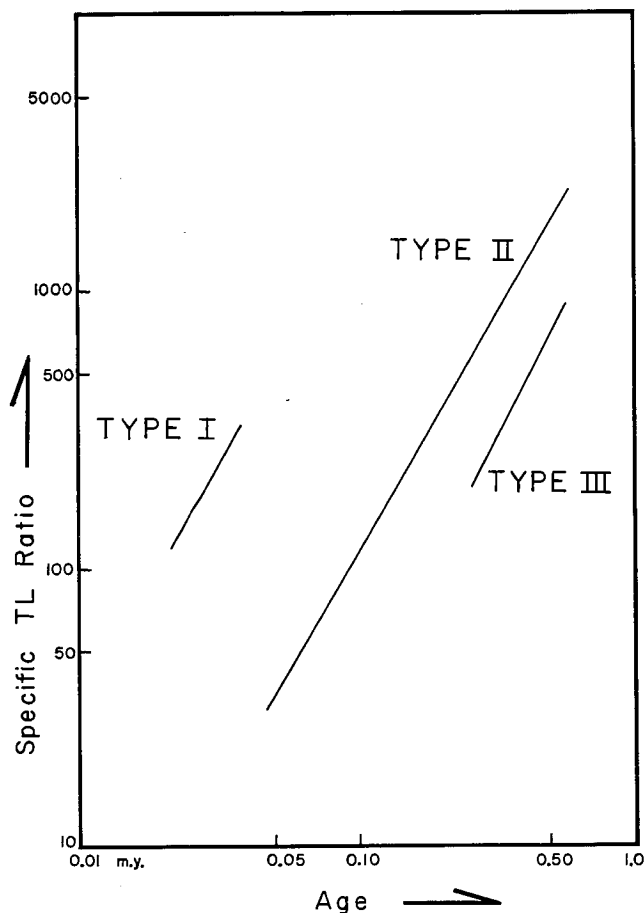


FIGURE 9.—Log-log plot of specific TL ratio, R , vs. age illustrating position and range of three sample types, Type I samples represent only those samples having lowest TL and radiometric age uncertainties.

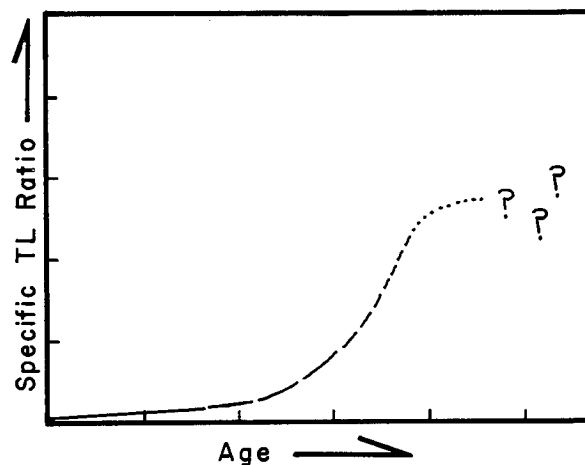


FIGURE 10.—Hypothetical development and saturation of the TL signal.

researchers. The geographic and petrochemical diversity of these samples has shown that it is not possible to simply class all basaltic rocks into one group for TL age dating. Further study into petrochemically dependent TL variations would significantly contribute to our understanding of the parameters which control such variations in TL; such work is essential if TL age dating is to ever achieve more than local usefulness.

Variations in TL glow-curve morphology and intensity were shown to be of key importance for the grouping and dating of the samples. However, these observed variations lead to perplexing questions regarding the degree of natural variability in the TL processes acting in naturally occurring dosimeter crystals. A systematic study of such variations in the TL behavior of samples from a wide range of host rocks would be extremely valuable for evaluating the petrochemical dependencies and limitations of TL dating.

Further work to define more accurately the relative contributions to the dose rate of radioelements within and outside the geologic dosimeter crystals would allow important refinements of the composite dose rate model. Such studies will require an accurate mineralogical characterization of the samples and suggest that microprobe analysis of all samples will soon become essential for all TL research.

At this point, however, it is important to recall some of the limitations inherent within the thermoluminescence method. Unlike traditional isotopic dating schemes whose nuclear decay constants are effectively oblivious to their chemical and physical environment, the TL accumulation and retention properties of a mineral are critically dependent upon its environmental conditions and upon changes in these conditions. An awareness of these dependencies and limitations must lead to the conclusion that the TL age-dating method has only limited geologic applicability. Its instability and vulnerability to heat, shock, recrystallization, "spontaneous annealing," and "anomalous fading" more than offset its major advantage of being able to use such ubiquitous minerals as quartz and the feldspars. Nonetheless, the method seems to have promising, if limited, applications to the dating of young volcanic rocks, but only where the K-Ar or ^{14}C methods are unusable. In such cases TL age dating may offer information that would not be obtainable by any other currently available method. If so, we should exploit the method where applicable but always bear in mind its limitations, prerequisite conditions, and inherent uncertainties.

Acknowledgments

At the conclusion of this thesis undertaking, I would like to extend special thanks to two advisers and friends who have provided invaluable encouragement and assistance over the last two years. Myron Best conceived the project and has offered continuing support and advice throughout its course; I am truly indebted to him for his assistance. Morris Petersen contributed encouragement and financial support at crucial times when the immediate prospects of success were less than excellent.

Rodd May generously allowed me the use of his TL lab at USGS, Menlo Park. This study would not have been possible without his aid and interest.

Alan R. Smith of Lawrence Berkeley Laboratories answered my naive questions about gamma-ray spectrometry and graciously performed U and Th analyses on several of my samples. W. P. Nash of the University of Utah generously donated the use of their microprobe facilities and assisted in the interpretation and computation of the results. George Ulrich,

USGS, Flagstaff, supplied the samples from the O'Neill and SP flows in the San Francisco volcanic field. Bart Kowallis collected the samples from California and Idaho. Lehi Hintze and Revel Phillips reviewed this manuscript and offered helpful suggestions for its improvement.

APPENDIX

SAMPLE	1 LNG73G001	2 LNG73G008	3 LNG73G009B	4 LNG73G012
SiO ₂	54.7	55.8	51.1	54.8
TiO ₂	1.93	1.29	1.71	1.98
Al ₂ O ₃	17.5	17.9	17.9	17.8
Fe ₂ O ₃	9.32	7.74	9.52	9.46
MnO	0.15	0.12	0.15	0.12
MgO	3.07	3.68	5.15	2.33
CaO	6.18	6.73	8.45	5.78
Na ₂ O	4.58	4.20	3.66	4.32
K ₂ O	2.23	2.07	1.73	2.25
P ₂ O ₅	0.54	0.41	0.63	0.57
LOI	0.05	0.00	0.09	1.12
TOTAL	100.25	99.94	100.09	100.53

CIPW Norms

Q	1.82	3.50		4.52
Or	13.21	12.30	10.30	13.42
Ab	38.94	35.74	31.21	36.96
An	20.61	24.01	27.37	22.97
Ne				
Di	5.44	5.60	8.70	1.95
Hy	11.42	12.43	9.38	11.35
Ol			4.59	
Mt	3.59	2.98	3.68	3.68
Il	3.67	2.46	3.27	3.81
Ap	1.29	0.98	1.50	1.35
TOTAL	99.99	100.00	100.00	100.01
An/(An+Ab)	0.35	0.40	0.47	0.38

1. Andesite, Long Valley Caldera, California
2. Andesite, Long Valley Caldera, California
3. High-alumina basalt, Long Valley Caldera, California
4. Andesite, Long Valley Caldera, California

SAMPLE	5 LNG73G014	6 LNG74G011	7 Flg-1	8 Flg-2
SiO ₂	51.7	49.5	58.2	57.8
TiO ₂	1.87	1.50	0.94	0.94
Al ₂ O ₃	17.4	18.0	15.5	14.9
Fe ₂ O ₃	10.08	9.53	6.98	6.93
MnO	0.16	0.14	0.12	0.14
MgO	4.39	6.53	4.35	5.00
CaO	7.85	9.76	6.89	7.69
Na ₂ O	4.08	3.27	3.96	3.72
K ₂ O	1.83	1.06	2.56	2.48
P ₂ O ₅	0.60	0.40	0.50	0.56
LOI	0.08	0.01	0.25	0.00
TOTAL	100.04	99.70	100.25	100.16

CIPW Norms

Q			5.99	5.69
Or	10.90	6.37	15.18	14.73
Ab	34.79	27.94	33.67	31.54
An	24.03	31.50	17.13	16.57
Ne				
Di	9.16	11.96	11.33	14.57
Hy	7.84	6.00	11.06	11.13
Ol	4.39	8.69		
Mt	3.89	3.70	2.69	2.67
Il	3.56	2.89	1.78	1.77
Ap	1.43	0.95	1.17	1.33
TOTAL	99.99	100.00	100.00	100.00
An/(An+Ab)	0.41	0.53	0.34	0.34

5. High-alumina basalt, Long Valley Caldera, California
6. High-alumina basalt, Long Valley Caldera, California
7. Basaltic andesite, O'Neill flow, San Francisco Volcanic field, Arizona
8. Basaltic andesite, SP flow, San Francisco Volcanic field, Arizona

SAMPLE	9 Ink-W1329	10 Ink-W1330	11 McC-W1121	12 Cmn-1
SiO ₂	46.8	46.1	45.5	47.9
TiO ₂	2.30	2.42	2.40	3.09
Al ₂ O ₃	15.2	15.4	14.9	12.6
Fe ₂ O ₃	13.27	13.40	14.19	17.58
MnO	0.19	0.19	0.21	0.26
MgO	8.07	7.82	8.21	3.78
CaO	10.25	10.11	10.02	7.50
Na ₂ O	1.91	1.94	2.39	3.01
K ₂ O	1.11	0.96	0.58	1.87
P ₂ O ₅	0.47	0.50	0.54	2.04
LOI	0.00	0.00	0.00	0.00
TOTAL	99.57	98.84	98.94	99.63

CIPW Norms

Q				3.30
Or	6.68	5.79	3.52	11.24
Ab	16.40	16.75	20.60	25.86
An	29.97	31.10	28.83	15.68
Ne				
Di	14.94	13.55	14.84	7.13
Hy	16.67	17.47	10.65	19.09
Ol	4.62	4.18	10.03	
Mt	5.16	5.25	5.56	6.85
Il	4.43	4.70	4.64	5.94
Ap	1.12	1.22	1.32	4.91
TOTAL	99.99	100.01	99.99	100.00
An/(An+Ab)	0.65	0.65	0.58	0.38

9. Olivine tholeiite, Inkorn, Idaho

10. Olivine tholeiite, Inkorn, Idaho

11. Olivine tholeiite, McCammon, Idaho

12. "Evolved" olivine tholeiite, Craters of the Moon, Idaho

SAMPLE	17 Zion-69	18 SG-33B	19 Whw-2*	20 Whw-6-3*
SiO ₂	50.4	48.0	45.5	47.8
TiO ₂	1.37	1.49	2.34	1.73
Al ₂ O ₃	15.2	15.0	13.5	14.2
Fe ₂ O ₃	9.00	13.00	11.97	11.37
MnO	0.15	0.17	0.18	0.17
MgO	8.07	8.10	10.84	10.48
CaO	8.62	9.73	10.65	10.18
Na ₂ O	3.55	3.15	3.08	3.64
K ₂ O	1.93	0.62	1.45	1.00
P ₂ O ₅	0.57	0.23	0.53	0.42
LOI	0.12	0.00	0.04	0.00
TOTAL	98.98	99.49	100.08	99.99

CIPW Norms

Q				
Or	11.61	3.70	8.72	5.96
Ab	30.53	27.00	13.23	22.52
An	20.24	25.38	18.96	24.06
Ne			6.30	
Di	15.64	17.89	25.05	19.31
Hy	0.10	3.81		2.87
Ol	14.36	13.76	17.26	16.56
Mt	3.52	5.06	4.67	4.40
Il	2.64	2.86	4.53	3.31
Ap	1.36	0.55	1.28	1.00
TOTAL	100.00	100.01	100.00	99.99
An/(An+Ab)	0.40	0.48	0.59	0.52

*Normalized to 100 percent total.

17. Hawaiite, Cedar City, Utah

18. Hawaiite, St. George, Utah

19. Basanite, Whitmore Wash, Grand Canyon, Arizona

20. Alkali olivine basalt, Whitmore Wash, Grand Canyon, Arizona

SAMPLE	13 Nel 1-B*	14 SG-81	15 Zion-20**	16 Zion-68
SiO ₂	46.0	46.0	52.7	49.9
TiO ₂	3.31	2.16	1.62	1.51
Al ₂ O ₃	14.0	13.7	16.1	14.3
Fe ₂ O ₃	16.28	12.04	9.03	10.95
MnO	0.21	0.17		0.16
MgO	6.75	9.86	6.20	9.18
CaO	9.45	10.72	7.59	9.17
Na ₂ O	2.54	2.98	3.87	2.82
K ₂ O	0.84	1.36	2.41	1.07
P ₂ O ₅	0.54	0.64	0.71	0.39
LOI	0.00	0.00		0.00
TOTAL	99.92	99.63	100.23	99.45

CIPW Norms

Q				
Or	5.02	8.22	14.30	6.43
Ab	21.75	15.90	32.87	24.22
An	24.72	19.58	19.46	23.43
Ne		4.72		
Di	15.63	24.97	11.02	16.20
Hy	14.20		7.77	14.88
Ol	4.70	16.11	6.33	6.73
Mt	6.32	4.77	3.48	4.26
Il	6.36	4.21	3.09	2.91
Ap	1.29	1.52	1.69	0.93
TOTAL	99.99	100.00	100.01	99.99
An/(An+Ab)	0.53	0.55	0.37	0.49

*Normalized by 100 percent total.

**Analyzed by M. G. Best (pers. comm., 1977).

13. Olivine tholeiite, Snake River Plain, Idaho

14. Alkali olivine basalt, St. George, Utah

15. Hawaiite, Zions National Park, Utah

16. Hawaiite, Zions National Park, Utah

SAMPLE	21 Whw-9*	22 Vulc-11*	23 U49*	24 Htn-18*
SiO ₂	47.3	47.2	44.7	47.2
TiO ₂	2.02	1.51	2.63	1.41
Al ₂ O ₃	14.0	14.5	14.4	13.9
Fe ₂ O ₃	12.04	11.92	12.84	11.22
MnO	0.17	0.18	0.17	0.17
MgO	9.91	10.40	10.39	11.65
CaO	10.24	10.10	9.89	10.22
Na ₂ O	2.76	2.88	2.96	2.89
K ₂ O	1.15	0.87	1.45	0.86
P ₂ O ₅	0.44	0.43	0.50	0.49
LOI	0.00	0.00	0.00	0.04
TOTAL	100.03	99.99	99.93	100.05

CIPW Norms

Q				
Or	6.86	5.19	8.71	5.14
Ab	22.50	22.77	14.50	21.49
An	22.49	24.44	22.14	22.55
Ne	0.51	0.87	5.19	1.53
Di	20.79	18.79	19.58	20.34
Hy				
Ol	17.26	19.41	18.58	20.72
Mt	4.66	4.62	5.01	4.35
Il	3.87	2.90	5.08	2.71
Ap	1.05	1.00	1.20	1.17
TOTAL	99.99	99.99	99.99	100.00
An/(An+Ab)	0.50	0.52	0.60	0.51

*Normalized by 100 percent total.

21. Alkali olivine basalt, Whitmore Wash, Grand Canyon, Arizona

22. Alkali olivine basalt, Vulcans Throne, Grand Canyon, Arizona

23. Basanite, Toroweap Valley, Grand Canyon, Arizona

24. Alkali olivine basalt, Uinkaret Plateau, Arizona

SAMPLE	25 Pav-51*	26 Pav-53	27 Pav-54A	28 Brd-6
SiO ₂	50.1	50.1	49.7	49.2
TiO ₂	1.36	1.40	1.33	1.54
Al ₂ O ₃	17.0	16.5	16.9	15.3
Fe ₂ O ₃	9.79	9.88	9.35	14.22
MnO	0.17	0.16	0.15	0.54
MgO	7.53	7.09	7.13	5.72
CaO	10.18	10.32	10.36	7.93
Na ₂ O	2.52	2.63	2.80	3.55
K ₂ O	1.10	1.11	1.17	1.17
P ₂ O ₅	0.29	0.32	0.28	0.33
LOI	0.00	0.00	0.08	0.01
TOTAL	100.04	99.51	99.25	99.51

CIPW Norms

Q				
Or	6.55	6.67	7.03	6.99
Ab	21.47	22.50	24.05	30.44
An	31.91	30.33	30.45	22.85
Ne				
Di	13.73	15.64	16.03	12.26
Hy	16.97	15.76	9.65	9.68
Ol	2.30	1.82	5.91	8.50
Mt	3.78	3.84	3.65	5.54
Il	2.60	2.68	2.56	2.96
Ap	0.69	0.76	0.67	0.79
TOTAL	100.00	100.00	100.00	100.01
An/(An + Ab)	0.60	0.57	0.56	0.43

*Normalized to 100 percent total.

25. Olivine tholeiite, Black Rock Desert, Utah

26. Olivine tholeiite, Black Rock Desert, Utah

27. Olivine tholeiite, Black Rock Desert, Utah

28. Sideromelane-palagonite tuff, Black Rock Desert, Utah

SAMPLE	29 Tbn-50	30 Cov-51	31 Cov-54	32 Cov-55
SiO ₂	49.0	55.6	56.0	60.9
TiO ₂	1.57	1.39	1.40	0.88
Al ₂ O ₃	16.3	15.6	15.7	15.4
Fe ₂ O ₃	12.06	9.53	9.52	6.25
MnO	0.19	0.15	0.14	0.10
MgO	7.14	4.06	4.08	2.78
CaO	9.46	6.92	6.74	5.33
Na ₂ O	3.07	3.64	3.05	2.82
K ₂ O	0.98	2.23	2.24	3.16
P ₂ O ₅	0.41	0.71	0.72	0.29
LOI	0.00	0.00	0.00	0.92
TOTAL	100.18	99.83	99.59	98.83

CIPW Norms

Q		5.82	9.25	16.78
Or	5.84	13.27	13.38	19.17
Ab	26.12	31.09	26.06	24.54
An	28.12	19.78	22.77	20.45
Ne				
Di	13.37	8.32	5.11	3.92
Hy	9.07	13.67	15.29	10.27
Ol	8.84			
Mt	4.66	3.69	3.70	2.46
Il	3.01	2.66	2.70	1.71
Ap	0.98	1.69	1.74	0.70
TOTAL	100.01	99.99	100.00	100.00
An/(An + Ab)	0.52	0.39	0.47	0.45

29. Olivine tholeiite, Black Rock Desert, Utah

30. Basaltic andesite, Cove Fort, Utah

31. Basaltic andesite, Cove Fort, Utah

32. Latite, Cove Fort, Utah

REFERENCES CITED

- Adams, J. A. S., and Gasparini, P., 1970, Gamma-ray spectrometry of rocks: Elsevier, New York, 295p.
- Aitken, M. J., 1968, Thermoluminescent dating in archaeology: Introductory review: In McDougall, D. J. (ed.), Thermoluminescence of geological materials: Academic Press, New York, p. 369-78.
- , 1974, Physics and archaeology, 2nd ed.: Oxford, New York, 291p.
- Aitken, M. J., and Bowman, S. G. E., 1975, Thermoluminescent dating: Assessment of alpha particle contribution: Archaeometry, v. 17, p. 132-38.
- Bailey, R. A., Dalrymple, G. B., and Lanphere, M. A., 1976, Volcanism, structure, and geochronology of the Long Valley Caldera, Mono County, California: Journal of Geophysical Research, v. 81, no. 5, p. 725-44.
- Bell, W. T., 1976, The assessment of the radiation dose-rate for thermoluminescence dating. Archaeometry, v. 18, p. 107-11.
- Berry, A. L., 1973, Thermoluminescence of Hawaiian basalts: Journal of Geophysical Research, v. 78, no. 29, p. 6863-67.
- Best, M. G., and Brimhall, W. H., 1974, Late Cenozoic alkalic basaltic magmas in the western Colorado Plateaus and the Basin and Range transition zone, USA, and their bearing on mantle dynamics: Geological Society of America Bulletin, v. 85, p. 1677-90.
- Best, M. G., and Hamblin, W. K., 1979, Origin of the northern Basin and Range Province: Implications from the geology of its eastern boundary: Geological Society of America Memoir 152.
- Cairns, T., 1976, Archaeological dating by thermoluminescence: Analytical Chemistry, v. 48, p. 266A-79A.
- Chayes, F., 1966, Alkaline and subalkaline basalts: American Journal of Science, v. 264, p. 128-45.
- Clark, E. E., 1977, Late Cenozoic volcanic and tectonic activity along the eastern margin of the Great Basin, in the proximity of Cove Fort, Utah: Brigham Young University Geology Studies, v. 24, pt. 1, p. 87-114.
- Dalrymple, G. B., and Doell, R. R., 1970, Thermoluminescence of lunar samples from Apollo 11: Proceedings of the Apollo 11 Lunar Science Conference, v. 3, p. 2081-92.
- Fleck, R. J., Anderson, J. J., and Rowley, P. D., 1975, Chronology of mid-Tertiary volcanism in High Plateaus region of Utah: In Anderson, J. J., Rowley, P. D., Fleck, R. J., and Nairn, A. E. M., Cenozoic geology of the southwestern High Plateaus of Utah: Geological Society of America Special Paper 160, p. 53-61.
- Garlick, G. F. J., Lamb, W. E., and Steigman, G. A., 1971, Thermoluminescence of lunar samples and terrestrial plagioclases: Proceedings of the Second Lunar Science Conference, v. 3, p. 2277-83.
- Geake, J. E., Walker, G., Telfer, D. J., Mills, A. A., and Garlick, G. F. J., 1973, Luminescence of lunar, terrestrial, and synthesized plagioclase, caused by Mn+2 and Fe+3: Proceedings of the Fourth Lunar Science Conference, v. 3, p. 3181-89.
- Holmes, R. D., Best, M. G., and Hamblin, W. K., 1978, Calculated strain rates and their implications for the development of the Hurricane and Toroweap faults, Utah and northern Arizona: U.S. Geological Survey, Earthquake Hazards Reduction Program, Summaries of Technical Reports.
- Hoover, J. D., 1974, Periodic Quaternary volcanism in the Black Rock Desert, Utah: Brigham Young University Geology Studies, v. 21, pt. 1, p. 3-72.
- Hwang, F. S. W., 1971, Thermoluminescence dating applied to volcanic lavas: Modern Geology, v. 2, p. 231-34.
- Hwang, F. S. W., and Goksu, H. Y., 1971, A further investigation on the thermoluminescence dating technique: Modern Geology, v. 2, p. 225-30.
- Irvine, T. N., and Baragar, W. R. A., 1971, A guide to the chemical classification of the common volcanic rocks: Canadian Journal of Earth Science, v. 8, p. 523-48.
- Leeman, W. P., Vitaliano, C. J., and Prinz, M., 1976, Evolved lavas from the Snake River Plain: Craters of the Moon National Monument, Idaho: Contributions to Mineralogy and Petrology, v. 56, p. 35-60.
- Luchitta, I., 1972, Early history of the Colorado River in the Basin and Range Province: Geological Society of America Bulletin, v. 83, p. 1933-48.
- May, R. J., 1975, Thermoluminescence dating of Hawaiian basalts: Ph.D. dissertation, Stanford University, Palo Alto, California, 157p.
- , 1977, Thermoluminescence dating of Hawaiian alkalic basalts: Journal of Geophysical Research, v. 82, no. 20, p. 3023-29.
- McDougall, D. J. (ed.), 1968, Thermoluminescence of geological materials: Academic Press, New York, 678p.
- McKee, E. D., and McKee, E. H., 1972, Pliocene uplift of the Grand Canyon region: Time of drainage adjustment: Geological Society of America Bulletin, v. 83, no. 7, p. 1923-32.
- Millard, H. T., Jr., 1976, Determination of uranium and thorium in USGS standard rocks by the delayed neutron technique: In Flanagan, J. F. (ed.), Descriptions and analyses of eight new USGS rock standards: U.S. Geological Survey Professional Paper 840, p. 61-65.
- Moore, R. B., Wolfe, E. W., and Ulrich, G. E., 1976, Volcanic rocks of the eastern and northern parts of the San Francisco volcanic field, Arizona: Journal of Research, U.S. Geological Survey, v. 4, no. 5, p. 549-60.

- Norrish, K., and Hutton, J. T., 1969, An accurate X-ray spectrographic method for the analysis of a wide range of geologic samples: *Geochimica et Cosmochimica Acta*, v. 33, p. 431-53.
- Slemmons, D. B., 1966, Cenozoic volcanism of the central Sierra Nevada, California: In Bailey, E. H. (ed.), *Geology of northern California*: California Division of Mines and Geology Bulletin 190.
- Struckless, J. S., Millard, H. T., Jr., Bunker, C. M., Nkomo, I. T., Rosholt, J. N., Bush, C. A., Huffman, C., Jr., and Keil, R. L., 1977, A comparison of some analytical techniques for determining uranium, thorium, and potassium in granitic rocks: *Journal of Research, U.S. Geological Survey*, v. 5, no. 1, p. 83-91.
- Walker, G. W., Flanagan, F. J., Sutton, A. L., Bastron, H., Berman, S., Dinnin, J. I., and Jenkins, L. B., 1976, Quartz latite (dellenite), QLO-1, from southeastern Oregon: In Flanagan, F. J. (ed.), *Descriptions and analyses of eight new USGS rock standards*: U.S. Geological Survey Professional Paper 840, p. 15-20.
- Wintle, A. G., 1973, Anomalous fading of thermoluminescence in mineral samples: *Nature*, v. 245, p. 143-44.
- Yoder, H. S., and Tilley, C. E., 1962, Origin of basaltic magmas: An experimental study of natural and synthetic rock systems. *Journal of Petrology*, v. 3, p. 342-532.

